

# Hybrid transfer-matrix FDTD method for layered periodic structures

Alexei Deinega,<sup>1,\*</sup> Sergei Belousov,<sup>1</sup> and Ilya Valuev<sup>2</sup>

<sup>1</sup>Russian Research Centre "Kurchatov Institute," Kurchatov sq. 1, Moscow 123182, Russia

<sup>2</sup>Joint Institute for High Temperatures of RAS, Izhorskaya, 13, bld. 2, Moscow 125412, Russia

\*Corresponding author: poblizosti@kintech.ru

Received December 10, 2008; revised February 3, 2009; accepted February 4, 2009;  
posted February 13, 2009 (Doc. ID 105203); published March 13, 2009

A hybrid transfer-matrix finite-difference time-domain (FDTD) method is proposed for modeling the optical properties of finite-width planar periodic structures. This method can also be applied for calculation of the photonic bands in infinite photonic crystals. We describe the procedure of evaluating the transfer-matrix elements by a special numerical FDTD simulation. The accuracy of the new method is tested by comparing computed transmission spectra of a 32-layered photonic crystal composed of spherical or ellipsoidal scatterers with the results of direct FDTD and layer-multiple-scattering calculations. © 2009 Optical Society of America

OCIS codes: 000.3860, 000.4430, 290.0290.

Frequency-domain computational methods are often applied for calculation of the photonic band structure. A plane-wave basis may be used either to solve the eigenvalue problem for an infinite crystal [1] or to obtain the transfer-matrix elements for finite-size slabs. The transfer matrix establishes a linear relation between coefficients of basis expansion of the wave incident on a structure with those of the transmitted or reflected waves. Knowing the transfer matrix for a single layer, it is easy to calculate optical properties for the structure with an arbitrary (including infinite) number and a combination of layers. In some cases it is favorable to employ basis functions different from plane waves to obtain the analytical solution for scattering from a single element composing the periodical structure. For example, in the case of spherical scatterers, spherical harmonics are used in the multiple-scattering method [2] for infinite crystals or in the layer-multiple-scattering method [3] for slabs. These methods also have a modification for slightly nonspherical elements [4]. All of the mentioned techniques are limited in applicability. Plane-wave methods cannot be applied to the absorbing photonic structures. If scatterers in the structure have a nonsymmetrical shape, the usage of three-dimensional (3D) multiple-scattering methods becomes problematic or very computationally demanding. Some techniques pursue the strategy of reducing the scattering problem to a lower dimension as performed in the real-space transfer-matrix method [5] or the plane-wave transfer-matrix method [6]. In these approaches the transfer matrix is calculated for each of the thin sublayers of the simulated structure, and then the total transfer matrix is found by applying an iterative multiplication procedure.

To briefly review the transfer-matrix definition [3], let us consider a single-layered planar periodic structure specified by primitive translations  $\mathbf{a}_1, \mathbf{a}_2$  in the  $xy$  plane. The corresponding reciprocal-lattice primitive vectors  $\mathbf{b}_1, \mathbf{b}_2$  satisfy the relation  $\mathbf{b}_i \mathbf{a}_j = 2\pi \delta_{ij}$ . Let an incident plane-wave having frequency  $\omega$  propagate in a homogeneous medium with electrical per-

mittivity  $\epsilon$  and magnetic permeability  $\mu$ . Its wave vector with the length  $q^2 = \mu\epsilon(\omega/c)^2$  can be represented as a sum of components parallel and normal to the layer,

$$\mathbf{q}_{\mathbf{g}}^{\pm} = \mathbf{k}_{\parallel} + \mathbf{g} \pm [q^2 - (\mathbf{k}_{\parallel} + \mathbf{g})^2]^{1/2} \mathbf{u}_z, \quad (1)$$

where  $\mathbf{k}_{\parallel}$  belongs to the first surface Brillouin zone formed by vectors  $\mathbf{b}_1$  and  $\mathbf{b}_2$ ;  $\mathbf{g} = m_1 \mathbf{b}_1 + m_2 \mathbf{b}_2$ ; and  $\mathbf{u}_z$  is the unit vector in the positive  $z$  direction. The signs  $+$  and  $-$  correspond to the waves propagating in positive and negative  $z$  directions, respectively. In the case of  $q^2 < (\mathbf{k}_{\parallel} + \mathbf{g})^2$ , Eq. (1) corresponds to a wave decaying in the  $z$  direction. Plane waves  $\{\exp(i\mathbf{q}_{\mathbf{g}}^s \mathbf{r}) \mathbf{u}_i\}$  with a given  $\mathbf{g}$  (or, equivalently, given  $m_1$  and  $m_2$ ), direction  $s = \pm$  and polarization ( $i = 1$  or  $i = 2$  for two possible polarizations) may be used as a basis for the electric (magnetic) field characterized by frequency and angle to the surface (or, equivalently, by  $q$  and  $\mathbf{k}_{\parallel}$ ),

$$\mathbf{E}_{q\mathbf{k}_{\parallel}}(\mathbf{r}) = \sum_{s=\pm} \sum_{i=1}^2 \sum_{\mathbf{g}} [E]_{\mathbf{g}i}^s \exp(i\mathbf{q}_{\mathbf{g}}^s \mathbf{r}) \mathbf{u}_i.$$

Here  $[E]_{\mathbf{g}i}^s$  are expansion coefficients, and the unit vectors  $\mathbf{u}_{1,2}$  form an orthonormal basis in the field polarization plane, which is normal to the propagation direction  $\mathbf{q}_{\mathbf{g}}^s$ . An interaction of a wave with the scattering layer is equivalent to the action of a linear operator in the coefficients space. For example, let the incident field propagate in the positive  $z$  direction with some fixed  $q$  and  $\mathbf{k}_{\parallel}$ . The coefficients of expansion  $[E]_{\mathbf{g}i}^{\pm}$  of the transmitted and the reflected waves are related with coefficients  $[E]_{\mathbf{g}'i'}^+$  of the incident wave by the transmission matrix elements  $M_{\mathbf{g}i, \mathbf{g}'i'}^{++}$  and the reflection matrix elements  $M_{\mathbf{g}i, \mathbf{g}'i'}^{-+}$ ,

$$[E]_{\mathbf{g}i}^{\pm} = \sum_{i'=1}^2 \sum_{\mathbf{g}'} M_{\mathbf{g}i, \mathbf{g}'i'}^{\pm+} [E]_{\mathbf{g}'i'}^+. \quad (2)$$

In a similar way we define the transmission and the reflection matrix elements  $M_{\mathbf{g}i, \mathbf{g}'i'}^{-+}$ ,  $M_{\mathbf{g}i, \mathbf{g}'i'}^{--}$  corre-

sponding to the incident plane-wave propagating in the negative  $z$  direction.

In the following we describe a technique for the calculation of the transfer matrix for an arbitrary layer using the finite-difference time-domain (FDTD) method. This approach has all the advantages of FDTD [7]; it is relatively simple to implement, it is suitable for arbitrary geometry and absorbing materials, it does not use linear algebra, and it avoids slow matrix operations. The numerical experiment geometry is shown in the inset of Fig. 1; for simplicity we consider the case of normal wave incidence ( $\mathbf{k}_{\parallel} = 0$ ) in the positive  $z$  direction. The simulation is restricted to a unit cell with periodic boundary conditions along the  $x$  and the  $y$  axes. The virtual total field/scattered field (TF/SF) [7] surface generates an incident plane-wave impinging the cell. Perfectly matched layer (PML) [7] boundary conditions absorb reflected and transmitted waves modeling the extension of the  $z$  direction to infinity. The experiment is performed until radiation totally leaves the structure. Planar detector arrays located in the front and at the back of the structure record field values during the numerical experiment. The transmitted and the reflected expansion coefficients  $[E]_{\mathbf{g}_i}^{\pm}$  are obtained by the Fourier transformation of the measured fields in the detector plane and time  $\mathbf{E}(t, x, y) \rightarrow \mathbf{E}(\omega, g_x, g_y)$ , projection to the polarization direction  $\mathbf{u}_i$  of interest, and multiplication by the phase  $\exp(-id\sqrt{\mu\epsilon(\omega/c)^2 - g_x^2 - g_y^2})$ , corresponding to the distance  $d$  between the detectors array and the central plane of the structure  $z = 0$ .

We perform simulations with the incident wave of fixed polarization  $i'$  and Bragg direction  $\mathbf{g}'$ , scanning vectors  $\mathbf{g}'$  up to some maximum absolute value  $g_{\max}$ . Then the system in Eq. (2) is solved for the unknowns  $M_{\mathbf{g}_i, \mathbf{g}'i'}^{++}$  and  $M_{\mathbf{g}_i, \mathbf{g}'i'}^{--}$  for each frequency  $\omega$  using the known incident field components  $[E_{in}]_{\mathbf{g}'i'}^{+}$  and the numerically obtained transmitted and reflected field components  $[E]_{\mathbf{g}_i}^{\pm}$ . To simplify Eq. (2), we construct the electric field  $\mathbf{E}(\mathbf{r}, t)$  of the incident wave so that it has only one nonzero component  $[E_{in}]_{\mathbf{g}'i'}^{+}$  for each fre-

quency  $\omega$ . To do this we use the technique taken from the spectral FDTD method [8],

$$\mathbf{E}(\mathbf{r}, t) = \text{Re}(\hat{\mathbf{F}}_{\omega}[A(\omega)\mathbf{u}_{i'}e^{iz\sqrt{\mu\epsilon(\omega/c)^2 - \mathbf{g}'^2}}]e^{i\mathbf{g}'\cdot\mathbf{r}}), \quad (3)$$

where  $\hat{\mathbf{F}}_{\omega}$  is the inverse Fourier transform,  $\mathbf{u}_{i'}$  is one of the polarization vectors normal to the full wave vector [Eq. (1)], and the frequency profile  $A(\omega)$  is selected broad enough to cover the frequency range of interest. The polarization basis is selected so that one of the components ( $\mathbf{u}_1$ ) is parallel to the  $xy$  plane. The expression for the magnetic field is obtained from Eq. (3) by replacing the polarization vector with the conjugated one,  $\mathbf{u}_{i'} \rightarrow \mathbf{u}_{3-i'}$ . In fact, since the matrix elements are identical for electric and magnetic components, for each polarization we employ in Eq. (2) that field component, which is parallel to the  $xy$  plane. This maximal possible alignment of the calculated field vector with the Yee grid reduces interpolation effects and is indeed found in practice to produce more-accurate numerical results for the matrix elements. The time-dependent signal of Eq. (3) is generated by the TF/SF surface and may be used to obtain the matrix elements simultaneously for a range of frequencies. Similar experiments with the waves propagating from the other side of the structure are used to obtain  $M_{\mathbf{g}_i, \mathbf{g}'i'}^{--}$  and  $M_{\mathbf{g}_i, \mathbf{g}'i'}^{++}$ . Symmetry in the scattering layer may be used to reduce the number of the scanned vectors  $\mathbf{g}'$  and incidence directions  $s$ .

Transfer-matrix elements, corresponding to the evanescent waves ( $q^2 < \mathbf{g}'^2$ ) may be neglected if the layers are relatively far apart from each other. Otherwise calculation of these matrix elements requires some precautions. Because of fast decay of the evanescent components in the  $z$  direction, the TF/SF surface and the detectors must be placed very close to the scattering structure (1–2 Yee cells apart). We also found that if the spectrum generated by the TF/SF surface incident wave has a substantial number of evanescent frequencies, the numerical value of the wave observed on the mesh does not accurately correspond to the desired analytical form supplied to the generating surface. The generated signal contains spurious components in the whole frequency range, irrespective of the mesh resolution. An additional numerical experiment in vacuum (without the scattering structure) is then needed to calculate the actual form of  $[E_{in}]_{\mathbf{g}'i'}^{+}$ . The spurious signals generated by the TF/SF surface may, fortunately, be well classified in three types. The first is the backward wave  $[E_{in}]_{\mathbf{g}'i'}^{-}$  that must also be calculated by the vacuum simulation and accounted for when obtaining the wave reflected from the layer. The second is the wave with the opposite vector  $\mathbf{g}'$ , having a very small (several magnitudes less than the direct one) but nonnegligible  $[E_{in}]_{\mathbf{g}'i'}^{+}$  component. The components with other vectors  $\mathbf{g} \neq \pm\mathbf{g}'$  do not appear in the incident wave because of the oscillating coefficient  $\exp(i\mathbf{g}'\cdot\mathbf{r})$  in Eq. (3). The third kind of spurious signal is the wave with the conjugated polarization  $[E_{in}]_{\mathbf{g}'3-i'}$ . As the incident field appears in fact to be a mixture of compo-

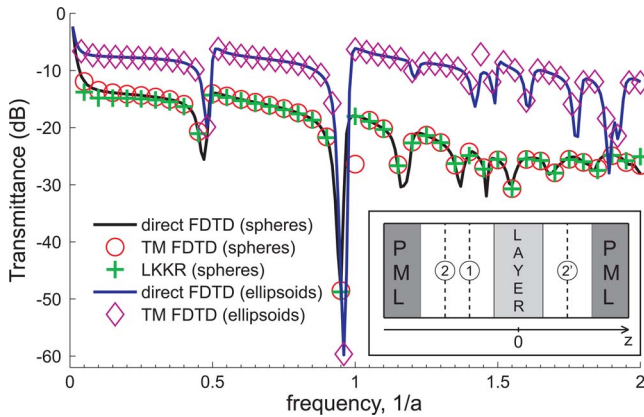


Fig. 1. (Color online) Transmittance of a 32-layered cubic lattice slab of conducting spheres or ellipsoids as scattering elements. Inset, scheme of the FDTD simulation geometry; 1, generating a (TF/SF) border; 2 and 2', detector arrays for reflected and transmitted signals.

nents, we solve Eq. (2) for  $M_{\mathbf{g}i,\mathbf{g}'i'}^{++}$  of the mixed modes simultaneously, after four numerical experiments with the incident waves  $\pm\mathbf{g}'$  and polarizations  $i' = 1, 2$ . This system of linear equations proves to be well conditioned and is easily solved numerically. The matrix elements  $M_{\mathbf{g}i,\mathbf{g}'i'}^{-+}$ ,  $M_{\mathbf{g}i,\mathbf{g}'i'}^{--}$  and  $M_{\mathbf{g}i,\mathbf{g}'i'}^{+-}$  for evanescent frequencies are found analogously.

We have tested our method by calculating the transmission of a photonic crystal slab consisting of 32 layers. Each layer is a planar square lattice of conducting ( $\epsilon=1.5$ ,  $\sigma=0.5$ ) spheres or ellipsoids of revolution with the revolution (shorter) semiaxis normal to the slab surface. The lattice period and the distance between layers are equal to unity, the sphere radius is 0.4, the longer ellipsoid semiaxis is 0.4, and the short one is 0.2. A mesh step was set to 0.05. To reduce the staircase effect we used the subpixel smoothing method for conducting materials [9,10]. For the frequency range considered, nine vectors  $\mathbf{g}'$  were sufficient; their number reduced to three if symmetry is taken into account,  $(m_1, m_2) = (0, 0)$ ,  $(1, 0)$ , and  $(1, 1)$ . To obtain the layer transfer matrix we perform ten FDTD simulations for a single layer, two runs for the vector  $\mathbf{g}' = (0, 0)$  (in vacuum and with the structure) and four runs for each of the two remaining vectors  $\mathbf{g}'$  (in vacuum and with the structure for each polarization). The multiplication procedure to calculate the whole 32-layer transfer matrix takes negligible computational effort compared to the FDTD simulation of a single layer. In Fig. 1 a comparison is presented between transmittance spectra results, obtained by our method, direct FDTD simulation, and the layer Korringa–Kohn–Rostoker (LKKR) method [3] (only for spheres with the same nine matrix elements). We consider the direct FDTD calculation of 32 layers to be the most accurate method for the task and measure a relative error of different methods (Fig. 2) with respect to it. Note that this direct calculation is much slower than our hybrid method. Poor convergence of the Chebyshev series for spherical Bessel functions affects the con-

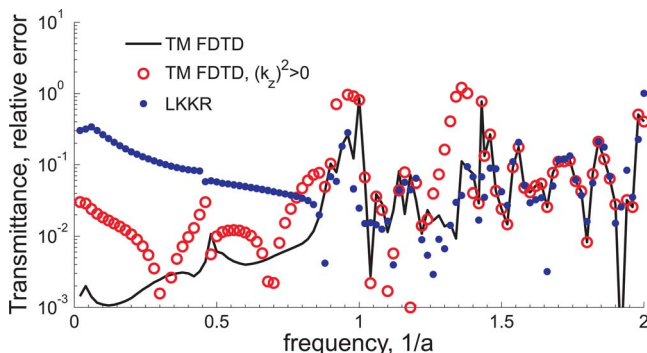


Fig. 2. (Color online) Relative error in transmittance of a 32-layered cubic lattice slab of conducting spheres measured with respect to the direct FDTD calculation. The case  $(k_z)^2 > 0$  corresponds to the neglect of evanescent modes in the hybrid transfer-matrix FDTD method.

vergence of the LKKR equations and leads to lower accuracy of the LKKR method at low frequencies. The results of our method are in good agreement with the others in the whole frequency range except for the values  $f \approx 1, \sqrt{2}, 2$ , where peaks of the relative error are observed. For these Bragg frequencies the  $z$  component of the wave vector for some of the measured waves is exactly zero, which leads to poor absorption of these waves by the PML [7]. The accuracy at these frequencies improves if the distance between the scattering layer and the PMLs is increased. As shown in Fig. 2, taking the evanescent waves into account improves the accuracy.

The transfer matrix for an obliquely incident wave may be calculated as described above by using the method of generating an obliquely incident plane-wave with the incident angle fixed for all frequencies [11]. In this case  $\mathbf{k}_{\parallel} \neq 0$  is different for each frequency and must enter the definition of the incident wave by Eq. (3). The FDTD method of the transfer-matrix calculation may also be used to compute the propagating and the evanescent eigenmodes for fixed  $\mathbf{k}_{\parallel}$  and  $\omega$  in an infinite 3D photonic crystal [3]. In this case, contrary to the fixed angle case, Bloch-periodic boundary conditions in  $x$  and  $y$  directions must be used as it was proposed in [8]. Note that compared to the direct eigenmode calculation by the FDTD [12], our method requires much less computation to resolve the whole band structure.

This work was partially supported by the research program 15 of the Russian Academy of Science (RAS). Computational resources were provided by the Distributed European Infrastructure for Supercomputing Applications (DEISA) in frames of the project Molecular Dynamics Simulation of the Condensed Matter and Plasmas (MDSCMP) of the DEISA Extreme Computing Initiative (DECI) program.

## References

1. K.-M. Ho, C. T. Chan, and C. M. Soukoulis, *Phys. Rev. Lett.* **65**, 3152 (1990).
2. A. Moroz, *Phys. Rev. B* **51**, 2068 (1995).
3. N. Stefanou, V. Yannopoulos, and A. Modinos, *Comput. Phys. Commun.* **132**, 189 (2000).
4. G. Gantzounis and N. Stefanou, *Phys. Rev. B* **73**, 035115 (2006).
5. J. B. Pendry, *J. Mod. Opt.* **41**, 209 (1994).
6. Z. Y. Li and L. L. Lin, *Phys. Rev. E* **67**, 046607 (2003).
7. A. Taflov and S. H. Hagness, *Computational Electrodynamics: The Finite Difference Time-Domain Method* (Artech House, 2005).
8. A. Aminian and Y. Rahmat-Samii, *IEEE Trans. Antennas Propag.* **54**, 1818 (2006).
9. A. Farjadpour, D. Roundy, A. Rodriguez, M. Ibanescu, P. Bermel, J. D. Joannopoulos, S. G. Johnson, and G. Burr, *Opt. Lett.* **31**, 2972 (2006).
10. A. Deinega and I. Valuev, *Opt. Lett.* **32**, 3429 (2007).
11. I. Valuev, A. Deinega, and S. Belousov, *Opt. Lett.* **33**, 1491 (2008).
12. S. Fan, P. Villeneuve, and J. Joannopoulos, *Phys. Rev. B* **54**, 11245 (1996).